# Reduction on High Level Waste Volume and Geological Repository Footprint with High Burn-up and High Thermal Efficiency of HTGR

Yuji Fukaya* and Tetsuo Nishihara

HTGR Hydrogen and Heat Application Research Center

Japan Atomic Energy Agency (JAEA)

4002 Narita-cho, Oarai-machi, Higashiibaraki-gun,Ibaraki 311-1393, Japan

*E-mail: fukaya.yuji@jaea.go.jp

Phone: +81-29-267-1919-3837

Fax: +81-29-266-7703

Total number of pages: 40

Total number of Tables: 9

Total number of Figures: 7

**Abstract**

Reduction on volume of High Level Waste (HLW) and footprint in a geological repository due to high burn-up and high thermal efficiency of High Temperature Gas-cooled Reactor (HTGR) has been investigated. A helium-cooled and graphite-moderated commercial HTGR was designed as a Gas Turbine High Temperature Reactor (GTHTR300), and that has particular features such as significantly high burn-up of approximately 120 GWd/t, high thermal efficiency around 50 %, and pin-in-block type fuel. The pin-in-block type fuel was employed to reduce processed graphite volume in reprocessing. By applying the feature, effective waste loading method for direct disposal is proposed in this study. By taking into account these feature, the number of HLW canister generations and its repository footprint are evaluated by burn-up fuel composition, thermal calculation and criticality calculation in repository.

As a result, it is found that the number of canisters and its repository footprint per electricity generation can be reduced by 60 % compared with Light Water Reactor (LWR) representative case for direct disposal because of the higher burn-up, higher thermal efficiency, less TRU generation, and effective waste loading proposed in this study for HTGR. But, the reduced ratios change to 20 % and 50 % if the long term durability of LWR canister is guaranteed. For disposal with reprocessing, the number of canisters and its repository footprint per electricity generation can be reduced by 30 % compared with LWR because of the 30 % higher thermal efficiency of HTGR.

KEYWORDS: HLW, footprint, high burn-up, HTGR, GTHTR300

## 1. Introduction

Recently, High Temperature Gas cooled Reactor (HTGR) has attracted a lot of attention from the viewpoint of safety (Ohashi, et al. 2011) especially from the Fukushima Daiichi nuclear power plant disaster in Japan in 2011. In other words, HTGR is expected as safe electric power sources to play a major role in the nuclear fuel cycle. However, its introduction effect research has not been performed enough, yet. Especially, issues concerning disposal of High Level radioactive Waste (HLW) should be resolved. Selection of repository sites have difficulties as Not In My Back Yard (NIMBY) problem, and the selected repository should be used effectively. In this context, HTGR has excellent features to reduce volume of HLW and its footprint in the repository, such as high burn-up, high thermal efficiency, and etc. The objectives of this study are to find the reduction effect due to the inherent features of HTGR comparing with Light Water Reactor (LWR), which is *de facto* standard of the Nuclear Power Generation (NPG).

As commercial HTGR, Gas Turbine High Temperature Reactor (GTHTR300) (Yan, et al.2003) have been developed with experiment of design, construction and operation of High Temperature Engineering Test Reactor (HTTR) (Saito, et al. 1994) at Japan Atomic Energy Agency (JAEA). GTHTR300 is designed as HTGR that has an annular type core with 600 MW thermal power and pin-in-block type fuel. The major specifications (Nakata, et al.2003) are listed in Table 1. The burn-up is 120 GWd/t in HTGR is triple of that 45GWd/t in LWR. This is expected to reduce HLW volume in direct disposal. The pin-in-block type fuel that is employed to reduce graphite volume should be processed in fuel reprocessing by withdrawing the fuel rods from the block. (Sumita et al. 2003) In this study, this feature is applied to direct disposal to reduce the

number of canister generation compared with the case disposing the Spent Fuels (SFs) with its fuel blocks. The thermal efficiency is significantly high value of around 50 %. The net value is 45.6 % in the standard design. It is expected that this contributes to reducing HLW volume not only for direct disposal but also for disposal of vitrified forms generated by reprocessing. In addition, higher efficiency of 50.4 % is also achievable with the reactor outlet coolant temperature of 950 °C and an advanced type of turbine blade composed of nickel based single-crystal (SC) nickel based alloy (Sato, et al. 2014).

In this study, the number of canister generation and its footprint in the repository per electricity generation for HTGR are evaluated with consideration for thermal transfer in a repository environment and compared with those of LWR. The calculation methods and conditions are described in Section 2. Burn-up characteristics and discharged fuel composition are described in Section 3. The number of canister generation and its footprint in the repository is evaluated for direct disposal and disposal with reprocessing in Section 4 and Section 5, respectively. The criticality is evaluated for direct disposal. Finally, the HLW volume reduction effect by HTGR is considered in Section 6.

In this study, LWR is represented by Pressurized Water Reactor (PWR) as same as Japan Atomic Energy Commission (JAEC).

Table1

## 2. Calculation Methods and Conditions

### 2.1 Scenario, Geological Repository Design and Safety Requirement

The scenario, repository design and specifications for disposal of PWR are referred from the report of JAEC (JAEC, 2004). According to this plan, the SFs are reprocessed

after 4 years from discharge, and the vitrified wastes are disposed after 50 years from reprocessing (after 54 years from discharge). Also for direct disposal, the SFs are disposed after 54 years to match the plan with reprocessing.

Two repositories are designed in the report based on the concept of KBS-3 (SKB, 2010a) proposed by SvenskKärnbränslehantering AB (SKB). Those are vertical emplacement and horizontal emplacement based on KBS-3V and KBS-3H, respectively. In this study, the vertical emplacement, which is the most achievable one, is selected for the reference case.

There are two parameters to determine the repository design: tunnel interval and waste package pitch. There are two limitations for those parameters from the safety requirement of structural integrity and maintenance of buffer function. For the first one, the limitations were evaluated by structural analysis (JAEC, 2004), and also employed in this study. For the second one, the maximum temperature in bentonite buffer is problematic. The buffer function that delays nuclide migration will be lost when the temperature exceeds 100 °C by thermal change of its property. The target value is set to be 90°C with considering uncertainties.(JAEC, 2004) The maximum temperature of bentonite is evaluated by time dependent thermal transfer calculations for the HTGR cases using ANSYS code (ANSYS, Inc. 2013), which solves the thermal equation by the finite element method with implicit time integral technique. The geometry of the thermal calculation is shown in Fig.1. If there is a margin from the target temperature of 90°C, the interval and pitch can be reduced as long as those are larger than the structural limitations. Here, the footprint per waste package can be defined as a product of the tunnel interval and waste package pitch. Like this, the footprint depends on the heat generation.

In addition, the waste must not achieve criticality in the repository forever. For direct disposal, the waste package includes residual $^{235}U$, and generated $^{239}Pu$ and $^{241}Pu$. The criticality is also evaluated for HTGR in this study as described in Section 2.2.

Fig.1

**2.2 Burn-up Calculation and Criticality Calculation in Repository**

To evaluate fuel burn-up composition, ORIGEN (Croff, 1983) code is used. ORIGEN code is burn-up code for many purposes, such as evaluation of the source of radioactive waste for storage and disposal, investigation on reactor strategy, etc. However, ORIGEN code cannot evaluate the neutron spectrum in a core, and that uses one energy group cross section libraries. For major reactors, libraries were already developed. Japan Nuclear Data Committee (JNDC) has been developed ORIGEN library of ORLIBJ40 (Okumura, et al. 2012) based on evaluated nuclear data of JENDL-4.0 (Shibata, et al. 2011). ORLIBJ40 includes libraries for LWRs and Fast Breeder Reactors (FBRs). For PWR calculations, the library named PWR47J40 in ORLIBJ40 is used in this study. However, libraries for HTGR do not exist.

The cross section library for HTGR is developed in this study. The scheme (Fukaya, et al. 2013) is as follows. ORIGEN libraries have two types of cross section library: Variable Actinide Cross Section (VAXS) library and static library. VAXS library depends on burn-up and includes the cross section of 20 nuclide-reactions for actinoid nuclides. The cross sections are provided by MVP code (Nagaya, et al. 2006) which is neutron transport calculation code based on the Monte Carlo method. For HTGR calculation, MVP code have an advantage to treat double heterogeneity effect, which is self-shielding effect caused by the complicated geometry with Coated Particle Fuel (CPF), by using statistical geometry model (Murata, et al. 1997). The MVP

calculations are performed with JENDL-4.0. MVP code provides effective cross section also for the static library. However, the effective cross sections provided by MVP code, for approximately 100 nuclides, are not enough for the static library that includes cross sections of approximately 1,400 nuclides. Then, not only JENDL-4.0, but also JEFF-3.1.2 (Koning, et al. 2011a), JENDL/A-96 (Nakajima, 1991), JEFF-3.1/A (Koning, et al. 2006) and TENDL-2011 (Koning, et al. 2011b) are used in order of descending priority. To treat these nuclides, infinite dilution cross sections with 108 energy group structure are generated by nuclear data processing code of NJOY (MacFarlane, et al. 2010). After that, the cross section is condensed by the 108 energy group neutron spectrum provided by MVP code. The cross sections and neutron flux from MVP code at Middle Of Cycle (MOC) are used for the static library. The geometry model for MVP calculation is shown in Fig. 2. This is two-dimensional model with reflective boundary for axial direction, and one-batch core to evaluate the burn-up characteristics from Begin Of Life (BOL) to End Of Life (EOL) for VAXS library. By this treatment, the burn-up characteristics of HTGR are reflected on almost all nuclides data in the ORIGEN library.

MVP code is also used to evaluate criticality safety in a geological repository for direct disposal. The values of upper side of three standard deviations are employed for the multiplication factor because the result of the Monte Carlo method has statistical distribution. The geometry model in the repository is shown in Fig. 3. The buffer is composed of 70 wt% of montmorillonite and 30 wt% of silica sand with moisture content of 7 %. The soft rock is represented by sandstone with moisture content of 30 %. The inside of the buffer region is described in Section 4.

Figs.2 and 3

## 3. Burn-up Characteristics and Discharged Fuel Composition

The burn-up composition and the decay heat are evaluated by using ORIGEN code for PWR and HTGR as described Section 2.2. The calculation conditions are listed in Table 2. The burn-up of HTGR is approximately 120 GWd/t, and it is almost 3 times larger than PWR's burn-up of 45 GWd/t although the burn-up days are almost same as that of PWR. In the same manner, specific power of HTGR is also larger than PWR's. The fuel enrichment of 14 wt% for HTGR is 3 times larger than PWR's 4.5 wt% because it should be proportional to the heat generation. This difference of design concepts also changes its burn-up fuel composition.

The fuel compositions are listed in Tables 3 and 4. For the compositions at 54 year from discharge, those are evaluated for SFs and reprocessed waste. The ratios where element is added into vitrified form are 0.442 % and 0.548 % for uranium and plutonium, respectively. For other actinoid element, the ratio of 100.0 % is assumed. (JNC, 2000) The fuel compositions are normalized by initial heavy metal inventory and heat generation, respectively. The residual $^{235}U$ inventory per initial heavy metal of 3.41 wt%IHM is 3 times larger than PWR's of 1.12 wt%IHM. (Here, IHM stands for initial heavy metal.) However, the value normalized heat generation of 0.285 kg/GWd is almost same as PWR's of 0.249 kg/GWd. TRans Uranium (TRU) nuclides inventory of HTGR of 0.151 kg/GWd is approximately half of PWR's of 0.273 kg/GWd in discharged fuel. For the reprocessing case, the amount of 0.022 kg/GWd is smaller than PWRs' of 0.028 kg/GWd.

Less TRU nuclides generation of HTGR, which is expected to reduce HLW, depends on the design concept and characteristics of reactor physics. TRU is composed of plutonium, Minor Actinoid (MA). MA includes neptunium, americium, and curium.

Neptunium generated from $^{235}U$ by 2 times of neutron capture reactions and β-decay, and its generation is proportional to burn-up because burn-up is also reaction of $^{235}U$. In addition, neptunium is not problematic from the viewpoint of decay heat because of the very long half-life of approximately 2 million years. Other TRU nuclides generated from $^{238}U$ by conversion reactions. The reactions are basically independent from the burn-up reaction although the neutron flux level is determined by the fission rate. The converted nuclide amount can be estimated by time integration of neutron capture reaction of $^{238}U$. Then, the inventory is proportional to the product of $^{238}U$ inventory, $^{238}U$ capture cross section, neutron flux level, and burn-up days. The $^{238}U$ inventory per heat generation of HTGR is one third of PWR's. However, $^{238}U$ capture cross section of HTGR is 3 times larger than PWR's. These two effects cancel each other out. The burn-up days are almost same as described above. The last, neutron flux level of HTGR is about half of PWR's because of the two times larger fission cross section of $^{235}U$. This effect contributes to reduce the TRU generation.

The decay heats per burn-up of PWR and HTGR are shown in Fig.4, and listed in Table 5 for actinoid nuclides showing major contribution for direct disposal and disposal with reprocessing. The decay heats of Fission Products (FPs) completely coincide because the difference of fission yield does not give a significant difference (Fukaya, et al.2008). For the case of direct disposal the decay heat of actinoid nuclides of HTGR of 6.22 W/GWd is 20 % lower than PWR's of 7.61 W/GWd at 54 years from discharged. Especially for $^{241}Am$, which shows the largest contribution, the decay heat of HTGR is 40 % lower than PWR's. The major part of $^{241}Am$ is generated by β-decay from $^{241}Pu$ after discharge. For the case of reprocessing, the decay heat of plutonium, which is recovered in the reprocessing, is small, and the decay heat of $^{241}Am$, which is

generated from $^{241}$Pu is also small. Although, the decay heat of $^{241}$Am that is generated during operation and cooling time of 4 years until reprocessing is dominant, and the decay heat of HTGR of 0.61 W/GWd is 30% smaller than PWRs' of 0.86 W/GWd. That of $^{244}$Cm for HTGR of 0.44 W/GWd is the almost same as PWR's of 0.46 W/GWd. The total value of HTGR of 1.11 W/GWd is 20% smaller than PWR's of 1.39 W/GWd.

Tables 2, 3,4 and 5 and Fig. 4

**4. Number of Waste Package Generation, Its Repository Footprint and Criticality in Repository for Direct Disposal**

As described Section 1, the feature of pin-in-block type fuel may be suitable to reduce HLW volume, and the high burn-up definitely contributes to reduce HLW volume. Then, the number of waste package generation is evaluated with considering these features in this study. The canister is assumed same as PWR based on KBS-3 concept by JAEC, but the material is carbon steel. The inner diameter is 864 mm, and the height is 4,300 mm. Here, we plan to withdraw fuel rods from the fuel blocks like the case with reprocessing (Sumita, et al. 2003), and insert the fuel rods into the canister as shown in Fig. 5. The fuel rod diameter is 26 mm, and the fuel rod length is 1,050 mm. The fuel rods can be contained 3,700 rods per canister, 925 rods per layer and 4 layers per canister. The fuel rods correspond to 9 % of a HTGR core, which has 41,040 fuel rods.

As a result, major specifications of HTGR waste for direct disposal determined as listed in Table 6, and those of PWR are also listed in the table. For PWR, 2 cases, 4 assemblies and 2 assemblies per canister, were investigated by JAEC. The residual $^{235}$U inventory of 21.8 kg/canister for HTGR is almost same as PWR 4 assemblies per

canister case of 20.6 kg/canister. The decay heat per canister at discharge from 54 years of HTGR of 1.12 kW/canister is 15 % smaller than the PWR's of 1.31 kW/canister. Furthermore, the fraction of FPs' decay heat, which decays faster than that of actinoid, is larger than PWR's. It is expected that footprint per canister of HTGR can be reduced from the 4 assemblies per canister case of PWR.

On this condition, the footprint per canister is evaluated for HTGR and PWR. The canister of PWR, contains 4 fuel assemblies per canister with thermal analysis. The tunnel interval is 32 m, and the waste package pitch is 10 m for PWR as same as reported by JAEC (JAEC, 2004). The tunnel interval is reduced to 24 m, and the waste package pitch is 8.5 m for HTGR with considering the heat generation. The interval and pitch are determined according to the structural limitations of 23.66 m and 8.232 m as reported by JAEC. The results are shown in Fig. 6. The maximum bentonite temperature of 89.8 °C for PWR shows a good agreement with that of 90 °C reported by JAEC. The maximum bentonite temperature of HTGR is 85.6 °C, and there is a margin of approximately 4 °C even though the footprint is reduced. The footprint of PWR with the case of 4 assemblies per canister is 320 $m^2$/canister. That of HTGR is 204 $m^2$/canister. In addition, that of PWR with the case of 2 assemblies per canister of 192 $m^2$/canister, which is almost the same as that of HTGR, is reported by JAEC, but the number of canisters becomes twice. The criticality is evaluated for HTGR and compared with the cases of PWR reported by JAEC.

For the criticality calculation of HTGR, the model inside of the buffer region is assumed as shown also in Fig. 5 in reference to the PWR model. The PWR model is also shown in Fig.7. The PWR model assumed that the canister made of carbon steel and structural material of fuel assembly made of zircaloy such as cladding, grid spacer

and etc. are completely corroded and flow out to outside of the buffer region. This assumption is realistic because the canister thickness is determined to endure the corrosion in the groundwater in 1,000 years (JNC, 2000), and the structure material will be dissolved in 7,600 years (JAEC, 2004). On the other hand, the fuel pellet spends a million years to be dissolved into the groundwater. After 10,000 years, the region inside of the buffer region is filled with groundwater and fuel pellets. (JAEC, 2004) The pellets distribute to realize the optimum moderation (moderator to fuel volume ratio is 3) from the viewpoint of criticality in the model as shown in Fig.7. Moreover, JAEC also assumed the case where poison effect of FPs is ignored. This assumption is reasonable with consideration of corrosion of fuel pellets. FPs would be dissolved faster than actinoid nuclides because many FPs have high solubility, and many actinoid nuclides have low solubility in general. In many cases, almost all nuclides of FPs are dissolved in groundwater, and the concentration of almost all nuclides of actinoid are saturated at the solubility and cannot be dissolved. It is difficult to predict the behavior of FPs in the repository.

On the contrary, the high durability of graphite material should be considered for the HTGR waste model. General Atomics (GA) evaluated the durability of Coated Fuel Particles (CFPs) in the repository. (Rodriguez, et al. 2003) The increase of failure fraction is evaluated by using Weibull distribution based on the weakest-link model with considering the thinning of SiC layer due to corrosion and internal pressure increase by helium gas generated by α-decay. As a result, it is found that the increase in failure fraction is negligible values less than $1\times10^{-4}$ even after a million years. The failure is induced by internal pressure increase, although that is accelerated by corrosion. The CFPs will be gradually failed and exposed to the groundwater. After that, the fuel

kernel made of $UO_2$ will be gradually corroded and flow out to out of the buffer region with remaining graphite structures. Then, we modeled the inside of the buffer region after canister corrosion with the remained fuel rods structure as shown in Fig.5. By the CFPs remaining integrity, the FP nuclides including gas are confined inside of the CFPs.

The results are shown in Fig. 8. In this study, the limitation of multiplication factor is set to be unity as same as JAEC report. However, criticality safety criteria with margin such as 0.95, which is also set by United States Nuclear Regulatory Commission (US NRC) regulatory for transportation and storage of SFs, should be employed in practice. The criticality changes are caused by decay of actinoid nuclides. The criticalities become low from 54 years to 100 years after discharge due to the decay of $^{241}$Pu. Later, the criticalities grow by the decay of $^{238}$Pu, $^{240}$Pu, and $^{241}$Am. The maximum criticalities are observed around $1\times10^4$ years for PWR because of the decay of $^{239}$Pu, whose half-life is 24,100 years. On the other hand, for HTGR, which generates TRU approximately half of PWR, the criticalities' behavior strongly depends on the decay of residual $^{235}$U, whose half-life is 703.5 million years, and the peak appliers around 10 million years.

The criticalities of PWR are referred from JAEC report (JAEC, 2004). The burn-up of the PWR fuel is set to be 40 GWd/t different from 45 GWd/t for thermal calculation, but the burn-up gives more conservative results for criticality. For the fuel assembly, 17x17 fuel assembly and initial uranium enrichment of 4.5 wt% are assumed. For the case of 4 fuel assemblies in a canister, the multiplication factor exceeds unity without considering FPs. Any treatments to remain subcriticality such as emplacement of neutron absorber should be necessary for this case. For the case of 2 fuel assemblies

in a canister, subcriticality is remained even the case without considering FPs. For HTGR, it is confirmed that subcriticality is remained all term even without considering FP. As described above, CFPs confine FPs. It is reasonable for HTGR that the poison effect of FPs is considered for criticality assessment in the repository. The largest margin for criticality is observed for the case of HTGR with FPs. If more criticality safety will be necessary to provide against particular accident scenarios, $B_4C$-C composite, which is employed as burnable poison in HTGR, and expected high durability for ground water as same as other graphite materials, can be employed as fuel rods binder and neutron absorber.

For the criticality safety of PWR, the estimation by JAEC gives very severe result. For example, SKB concluded that the multiplication factor can be limited lower than 0.95 even with the case of 4 fuel assemblies in a canister by the limitation of initial uranium enrichment and burn-up. (SKB, 2010b) For the case without poison effect of FPs, the design value of JAEC, initial uranium enrichment of 4.5% and burn-up of 45 GWd/t, can be applied the safety criteria.

SKB assumed the 15x15 type (F15x15AFA3G) fuel assembly. However, the fuel assembly is selected as representative one because it is most reactive compared with other types of fuel assembly including 17x17 type. For the condition, groundwater flooding into canister is assumed, but any corrosion of canister and/or fuel assembly is not assumed. This difference leads to the discrepancy between the criticality safety estimations.

As described above, JAEC employed the disposal canister concept based on SKB concept. The canister of the original SKB concept is surrounded by copper shell, which has high durability for 200,000 years (SKB, 1999) with quality of ground water

in Sweden. JAEC did not employ the copper shell concept because there is no guarantee of the high durability with the quality of ground water in Japan. (JAEC, 2004) In this situation, the corrosion model proposed by JAEC is reasonable.

In addition, the fuel blocks whose fuel rods are removed can be disposed as Low Level radioactive Waste (LLW). Only the radioactivity of $^{14}C$, which is Activation Product (AP) generated by conversion from $^{14}N$ and $^{13}C$, is problematic to satisfy a limitation of disposal in the site of LLW. The radioactivity was evaluated, and it was confirmed that the fuel blocks can be disposed in LLW site. (Sumita, et al. 2003). Moreover, the fuel blocks can be recycled by reuse of blocks after heat treatment to anneal out radiation damage or reconstituting fuel block by crushing and jet milling irradiated blocks to fine powder. (Windes, et al. 2007)

Table 6 and Figs. 5, 6, 7 and 8

## 5. Number of Vitrified Waste Generation and Its Repository Footprint with Reprocessing

The number of vitrified waste generation and its repository footprint with reprocessing for PWR were also evaluated (JAEC, 2004). Footprint of 90.0 $m^2$/canister was evaluated with waste pitch of 7.5 m and tunnel interval of 12.0 m in the case with soft rock and vertical emplacement. The layout is determined from the viewpoint of structural integrity. The maximum temperature in the bentonite buffer is 71 °C, which has a large surplus margin from a target of 90 °C. Therefore, the footprint per canister cannot be reduced if the decay heat from the waste would be reduced.

The condition to evaluate the number of vitrified waste was set to be uranium inventory of 0.8 ton per canister for PWR in the feasibility study. The inventory was determined by limitations from the viewpoint of fabrication of the vitrified form, its

storage and disposal. Major specifications and the limitations for Japanese vitrified waste model (JNC, 2000, and Inagaki et al. 2009) are listed in Table 7. The volume of glass is designed to be 150 liter/canister. The limitation of heat generation rate for storage to 2.3 kW/canister is employed to remain temperature of waste lower than 500 °C during storage to prevent the phase transmutations such as crystallization and liquid-liquid phase separation at elevated temperatures by decay heat. The limitation of heat generation rate for disposal to 0.35 kW/canister is employed to remain the temperature of bentonite buffer lower than 100 °C as described Section 2.1. The limitation for content of waste oxides, FP oxide and actinide oxide, to 20 wt% is determined from the viewpoint of radioactive nuclides confinement. The limitation for content of $MoO_3$ to 1.5 wt% is employed to prevent formation of Mo-rich phase, which is called yellow phase and degrade chemical durability of the vitrified form. The limitation for content of noble metals to 1.25 wt% is employed not to short the lifetime of Liquid Fed Ceramic Melter (LFCM). Since noble metals such as Ru, Rh, and Pd are insoluble in the borosilicate waste glass matrix, they tend to form separate phases of $RuO_2$ and Pd-Rh-Te alloys in the molten glass. These phases tend to accumulate at the melter bottom to form electrical short circuits, which cause power dissipation and electrode corrosion leading to a shortening of the melter lifetime.

The calculated vitrified waste specifications are listed in Table 8. The heavy metal inventory of HTGR of 0.33 t/canister is 40 % of PWR's of 0.79 t/canister. However, the amount of waste oxide contained in the canister of 8.6 wt% for HTGR is larger than PWR's of 8.3 wt% because plutonium and uranium are recovered and never disposed with reprocessing. The contained amount of waste oxide is determined by the limitation of heat generation of 2.3 kW/canister at fuel fabrication both for PWR and

HTGR. Other limitations are not problematic both for PWR and HTGR. For heat generation at the disposal of 0.37 kW/canister for HTGR, that slightly exceeds from the limitation to 0.35 kW/canister. However, it is not also problematic with considering the large surplus margin of repository design as described above.

## 6. Consideration on HLW Volume and Footprint Reduction Effect of HTGR

Tables 7 and 8

In this study, burn-up fuel composition and decay heat reflected the characteristics of HTGR design are evaluated, and the number of canister generation for direct disposal and disposal with reprocessing is evaluated. For direct disposal, the footprint in the repository is also evaluated with thermal calculations. In this section, the number of canisters and footprint in repository per electricity generation are evaluated and compared with those of PWR.

The result is listed in Table 9 with the major specification of reactor and fuel, and the result of Section 4 and Section 5. The burn-up of HTGR is almost 3 times higher than PWR's, and the thermal efficiency of HTGR is 30 % higher than PWR's. Owing to the higher burn-up, higher thermal efficiency, and the effective waste loading method proposed in this study, the number of canister generation of 1.20 canister/TWeh for HTGR is the lowest compared with the 2 assemblies and 4 assemblies per canister cases of PWR for direct disposal. It is reduced by 60 % from 2 assemblies per canister case of PWR of 2.92 canister/TWeh, and reduced by 20 % from 4 assemblies per canister case of PWR of 1.46 canister/TWeh. The footprint per electricity generation of 244.0 $m^2$/TWeh for HTGR is the lowest compared with PWR's cases. It is reduced by 60 % from 2 assemblies per canister case of PWR of 560.1 $m^2$/TWeh, and reduced by

50 % from 4 assemblies per canister case of PWR of 466.8 $m^2$/TWeh. The effective reduction of footprint per electricity generation is also owing to small footprint per canister of HTGR because of the low decay heat with the less TRU generation. That of 204 $m^2$/canister for HTGR is almost same as 2 assemblies per canister case of PWR of 192 $m^2$/canister. Comparing with the case of 4 assemblies per canister of 320 $m^2$/canister, it is reduced by 40 %. Subcriticality of repository is sufficiently remained for the direct disposal of HTGR. However, 4 assemblies per canister case of PWR achieves criticality without considering poison effect of FPs. In Japan, 2 assemblies per canister case should be the representative case of PWR with considering criticality safety in repository. On the other hands, 4 assemblies per canister case of PWR can be acceptable if the long term durability of canister is guaranteed.

For the disposal with reprocessing, the number of canister generation and repository footprint per electricity generation of HTGR are reduced by 30 % because of the 30 % higher thermal efficiency. The number of canister generation is determined by the heat generation limitation at vitrified form fabrication, and a major part of decay heat is generated from FPs, which is proportional to burn-up. The number per electricity generation is reduced with the higher thermal efficiency. The repository footprint per canister is determined by the structural limitation, and does not depend on heat generation. If other disposal ways such as horizontal emplacement based on the KBS-3H concept is employed and/or scenario of reprocessing and disposal is changed, less TRU generation of HTGR contributes to reduce the footprint in repository.

In addition, the economic analyses of the proposed waste loading method for HTGR spent fuel is necessary in the future, to evaluate the cost change of electricity generation.

Table 9

## 7. Conclusions

To investigate the introduction effect of HTGR for back-end problems, number of waste package generation and footprint in a geological repository are evaluated, and compared with LWR. LWR is represented by PWR. The repository design is based on the KBS-3V concept.

To evaluate burn-up fuel composition reflecting HTGR characteristics by ORIGEN code, ORIGEN library for HTGR is generated by criticality calculation with MVP code and infinite dilution cross section generation with NJOY code. For direct disposal, the repository design is determined by thermal calculation with ANSYS code to satisfy the limitation for maximum bentonite temperature. The criticality safety is assessed by using MVP code. To realize effective disposal, we proposed the new disposal method of HTGR that disposes only fuel rods.

For disposal with reprocessing, the number of waste package generation is evaluated with considering the limitation for vitrified form fabrication and its disposal. However, the footprint per canister of HTGR does not change with that of LWR because that is determined only by structural integrity of the repository.

As a result, it is found that the number of canisters and its repository footprint per electricity generation can be reduced by 60 % compared with LWR representative case for direct disposal because of the higher burn-up, higher thermal efficiency, less TRU generation, and effective waste loading proposed in this study for HTGR. However, if the long term durability of canister is guaranteed, 4 assemblies per canister case of PWR can be acceptable, and the number of canister and its repository footprint can be reduced by 20 % and 50 %, respectively, compared with LWR case. For disposal with reprocessing, the number of canister and its repository footprint per electricity

generation can be reduced by 30 % compared with LWR because of the 30 % higher thermal efficiency of HTGR.

**Acknowledgement**

The authors appreciate Dr. J. Sumita of JAEA who is an expert in back-end of HTGR, and provided valuable comments, and Mr. Y. Inada of JAEA who assist to use CAE tools for thermal calculations. The authors also appreciate Dr. M. Goto of JAEA who provides valuable comment for reactor physics of HTGR.

**List of Tables and Figures**

Table 1 Major specifications of GTHTR300

| Item | Value |
|---|---|
| Thermal power (MWt) | 600 |
| Thermal efficiency (%) | 45.6 |
| Uranium inventory (t) | 7.09 |
| $^{235}$U enrichment (wt%) | 14 |
| Fuel particle | SiC coated particle |
| Kernel diameter (μm) | 550 |
| Particle diameter (μm) | 1,010 |
| Particle packing fraction (%) | 28.5 |
| Block across flat (mm) | 410 |
| Fuel rod numbers | 57 |
| Fuel rod diameter (mm) | 26 |
| Coolant hole diameter (mm) | 39 |
| Burnable poison | B4C-C composite |
| Block height (mm) | 1,050 |
| Cycle length (days) | 706.0 |
| Number of batch | 2 |
| Discharge burn-up (GWd/t) | 119.5 |

Y. Fukaya:
Reduction on High Level Waste and Geological Repository Footprint with High Burn-up and High Thermal Efficiency of HTGR

Table 2 Condition of burn-up calculations

| | PWR | HTGR |
|---|---|---|
| Enrichment (wt%) | 4.5 | 14 |
| Specific power (MW/t) | 38 | 84.63 |
| Burn-up days (day) | 1184.21 | 1412.09 |
| Burn-up (GWd/t) | 45 | 119.5 |
| Neutron Flux at MOC ($cm^{-2}s^{-1}$) | $3.02\times10^{14}$ | $1.47\times10^{14}$ |
| Capture cross section of $^{238}U$ at MOC (barn) | 0.88 | 3.28 |
| Fission cross section of $^{235}U$ at MOC (barn) | 33.68 | 59.30 |

Y. Fukaya:

Reduction on High Level Waste and Geological Repository Footprint with High Burn-up and High Thermal Efficiency of HTGR

Table 3 Fuel compositions per initial heavy metal (wt%IHM)

| | PWR | | | | HTGR | | | |
|---|---|---|---|---|---|---|---|---|
| | Fresh | Discharged | at 54 years | at 54 years with reprocessing | Fresh | Discharged | at 54 years | at 54 years with reprocessing |
| $^{234}U$ | 0.00 | 0.00 | 0.01 | 0.00 | 0.00 | 0.00 | 0.03 | 0.00 |
| $^{235}U$ | 4.50 | 1.12 | 1.12 | 0.00 | 14.00 | 3.41 | 3.41 | 0.02 |
| $^{236}U$ | 0.00 | 0.57 | 0.57 | 0.00 | 0.00 | 1.79 | 1.80 | 0.01 |
| $^{238}U$ | 95.50 | 92.43 | 92.43 | 0.41 | 86.00 | 80.80 | 80.80 | 0.36 |
| $^{237}Np$ | 0.00 | 0.06 | 0.07 | 0.07 | 0.00 | 0.13 | 0.15 | 0.14 |
| $^{238}Pu$ | 0.00 | 0.03 | 0.02 | 0.00 | 0.00 | 0.08 | 0.05 | 0.00 |
| $^{239}Pu$ | 0.00 | 0.63 | 0.64 | 0.00 | 0.00 | 0.61 | 0.63 | 0.00 |
| $^{240}Pu$ | 0.00 | 0.25 | 0.25 | 0.01 | 0.00 | 0.34 | 0.36 | 0.01 |
| $^{241}Pu$ | 0.00 | 0.18 | 0.01 | 0.00 | 0.00 | 0.34 | 0.02 | 0.00 |
| $^{242}Pu$ | 0.00 | 0.07 | 0.07 | 0.00 | 0.00 | 0.25 | 0.25 | 0.00 |
| $^{241}Am$ | 0.00 | 0.01 | 0.16 | 0.03 | 0.00 | 0.01 | 0.30 | 0.06 |
| $^{243}Am$ | 0.00 | 0.01 | 0.01 | 0.01 | 0.00 | 0.04 | 0.04 | 0.04 |
| Total of U | 100.00 | 94.12 | 94.13 | 0.42 | 100.00 | 86.00 | 86.03 | 0.38 |
| Total of TRU | 0.00 | 1.23 | 1.23 | 0.12 | 0.00 | 1.80 | 1.80 | 0.26 |
| Total | 100.00 | 95.37 | 95.37 | 0.54 | 100.00 | 87.84 | 87.84 | 0.65 |

Table 4 Fuel compositions per burn-up (kg/GWd)

| | PWR | | | | HTGR | | | |
|---|---|---|---|---|---|---|---|---|
| | Fresh | Discharged | at 54 years | at 54 years with reprocessing | Fresh | Discharged | at 54 years | at 54 years with reprocessing |
| $^{234}$U | 0.000 | 0.000 | 0.002 | 0.000 | 0.000 | 0.000 | 0.002 | 0.000 |
| $^{235}$U | 1.000 | 0.249 | 0.249 | 0.001 | 1.172 | 0.285 | 0.285 | 0.001 |
| $^{236}$U | 0.000 | 0.127 | 0.127 | 0.001 | 0.000 | 0.150 | 0.150 | 0.001 |
| $^{238}$U | 21.222 | 20.539 | 20.539 | 0.091 | 7.197 | 6.761 | 6.761 | 0.030 |
| $^{237}$Np | 0.000 | 0.014 | 0.016 | 0.015 | 0.000 | 0.011 | 0.013 | 0.012 |
| $^{238}$Pu | 0.000 | 0.006 | 0.004 | 0.000 | 0.000 | 0.006 | 0.004 | 0.000 |
| $^{239}$Pu | 0.000 | 0.141 | 0.143 | 0.001 | 0.000 | 0.051 | 0.052 | 0.000 |
| $^{240}$Pu | 0.000 | 0.055 | 0.055 | 0.001 | 0.000 | 0.029 | 0.030 | 0.001 |
| $^{241}$Pu | 0.000 | 0.039 | 0.003 | 0.000 | 0.000 | 0.028 | 0.002 | 0.000 |
| $^{242}$Pu | 0.000 | 0.015 | 0.015 | 0.000 | 0.000 | 0.021 | 0.021 | 0.000 |
| $^{241}$Am | 0.000 | 0.001 | 0.035 | 0.008 | 0.000 | 0.001 | 0.025 | 0.005 |
| $^{243}$Am | 0.000 | 0.003 | 0.003 | 0.003 | 0.000 | 0.004 | 0.004 | 0.004 |
| Total of U | 22.222 | 20.916 | 20.918 | 0.092 | 8.368 | 7.197 | 7.200 | 0.032 |
| Total of TRU | 0.000 | 0.273 | 0.274 | 0.028 | 0.000 | 0.151 | 0.151 | 0.022 |
| Total | 22.222 | 21.193 | 21.193 | 0.120 | 8.368 | 7.351 | 7.351 | 0.054 |

Table 5 Decay heat per bun-up of major actinoid nuclides at 54 years from discharge (W/GWd)

| | PWR | | HTGR | |
|---|---|---|---|---|
| | Direct disposal | Disposal with reprocessing | Direct disposal | Disposal with reprocessing |
| $^{238}$Pu | 2.42 | 0.02 | 2.53 | 0.02 |
| $^{239}$Pu | 0.27 | 0.00 | 0.10 | 0.00 |
| $^{240}$Pu | 0.39 | 0.01 | 0.21 | 0.01 |
| $^{241}$Am | 4.01 | 0.86 | 2.89 | 0.61 |
| $^{243}$Am | 0.02 | 0.02 | 0.02 | 0.02 |
| $^{244}$Cm | 0.46 | 0.46 | 0.44 | 0.44 |
| Total | 7.61 | 1.39 | 6.22 | 1.11 |

Y. Fukaya:
Reduction on High Level Waste and Geological Repository Footprint with High Burn-up and High Thermal Efficiency of HTGR

Table 6 Major specifications of waste package for direct disposal

| | PWR | | HTGR |
|---|---|---|---|
| Fuel amount contained per canister | 2 assemblies | 4 assemblies | 3,700 rods |
| Heavy metal inventory (t/canister) | 0.92 | 1.84 | 0.64 |
| Residual $^{235}$U inventory (kg/canister) | 10.3 | 20.6 | 21.8 |
| Decay heat at 54 years from discharge (kW/canister) | 0.66 | 1.31 | 1.12 |

Y. Fukaya:
Reduction on High Level Waste and Geological Repository Footprint with High Burn-up and High Thermal Efficiency of HTGR

Table 7 Major specifications and limitations for Japanese vitrified waste model

| Items | Values |
|---|---|
| Materials | |
| Matrix | Borosilicate glass |
| Canister | Stainless steel |
| Dimensions | |
| Diameter (mm) | 430 |
| Height (mm) | 1,340 |
| Weights | |
| Glass (kg/canister) | 400 |
| Glass including canister (kg/canister) | 500 |
| Volume of glass(liter/canister) | 150 |
| Vitrification melter type | Liquid Fed Ceramic Melter (LFCM) |
| Limitations | |
| Heat generation rate for storage period (kW/canister) | ＜ 2.3 |
| Heat generation rate for disposal period (kW/canister) | ＜ 0.35 |
| Waste oxides content (wt%) | ＜ 20 |
| $MoO_3$ content (wt%) | ＜ 1.5 |
| Noble metals content (wt%) | ＜ 1.25 |

Y. Fukaya:
Reduction on High Level Waste and Geological Repository Footprint with High Burn-up and High Thermal Efficiency of HTGR

Table 8 Calculated specifications of vitrified waste for each reactor type

| | PWR | HTGR |
|---|---|---|
| Heavy metal inventory (t/canister) | 0.79 | 0.33 |
| Heat generation at vitrified form fabrication (kW/canister) | 2.30 | 2.30 |
| Heat generation at disposal (kW/canister) | 0.34 | 0.37 |
| Waste oxide content (wt%) | 8.3 | 8.6 |
| $MoO_3$ content (wt%) | 1.2 | 1.1 |
| Noble metal (Ru,Rh,Pd) content (wt%) | 0.8 | 0.8 |

Y. Fukaya:
Reduction on High Level Waste and Geological Repository Footprint with High Burn-up and High Thermal Efficiency of HTGR

Table 9 Calculated specifications of waste package
for direct disposal and disposal with reprocessing

| | PWR | | HTGR |
|---|---|---|---|
| Specifications | | | |
| Burn-up (GWd/t) | 45 | | 119.5 |
| Thermal efficiency (%) | 34.5 | | 45.6 |
| Heavy metal inventory per electricity generation (t/TWeh) | 2.684 | | 0.765 |
| Direct disposal | 2 assemblies in a canister | 4 assemblies in a canister | |
| Heavy metal inventory per canister (t/canister) | 0.920 | 1.840 | 0.639 |
| Number of canisters per electricity generation (canister/TWeh) | 2.92 | 1.46 | 1.20 |
| Repository footprint per canister ($m^2$/canister) | 192 | 320 | 204 |
| Repository footprint per electricity generation ($m^2$/TWeh) | 560.1 | 466.8 | 244.0 |
| Disposal with reprocessing | | | |
| Heavy metal inventory per canister (t/canister) | 0.790 | | 0.330 |
| Number of canisters per electricity generation (canister/TWeh) | 3.40 | | 2.32 |
| Repository footprint per canister ($m^2$/canister) | 90 | | 90 |
| Repository footprint per electricity generation ($m^2$/TWeh) | 305.8 | | 208.5 |

Y. Fukaya:
Reduction on High Level Waste and Geological Repository Footprint with High Burn-up and High Thermal Efficiency of HTGR

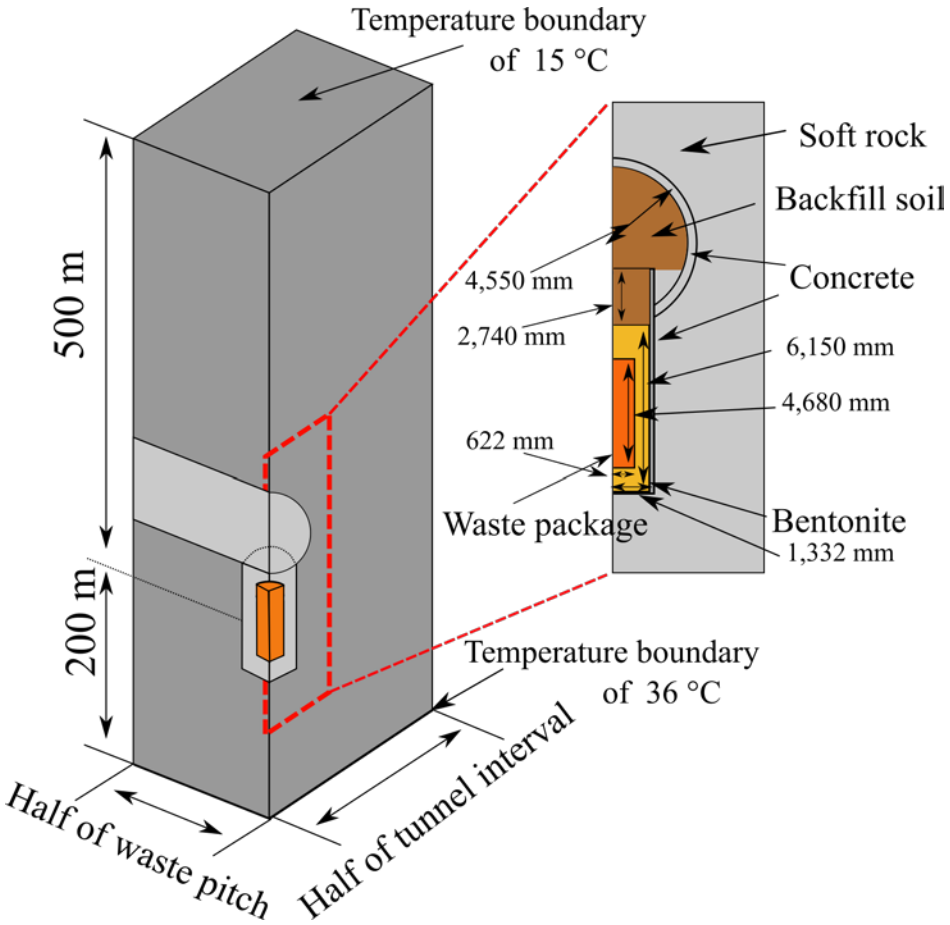

Fig.1 Geometry of thermal calculation

Y. Fukaya:
Reduction on High Level Waste and Geological Repository Footprint with High Burn-up and High Thermal Efficiency of HTGR

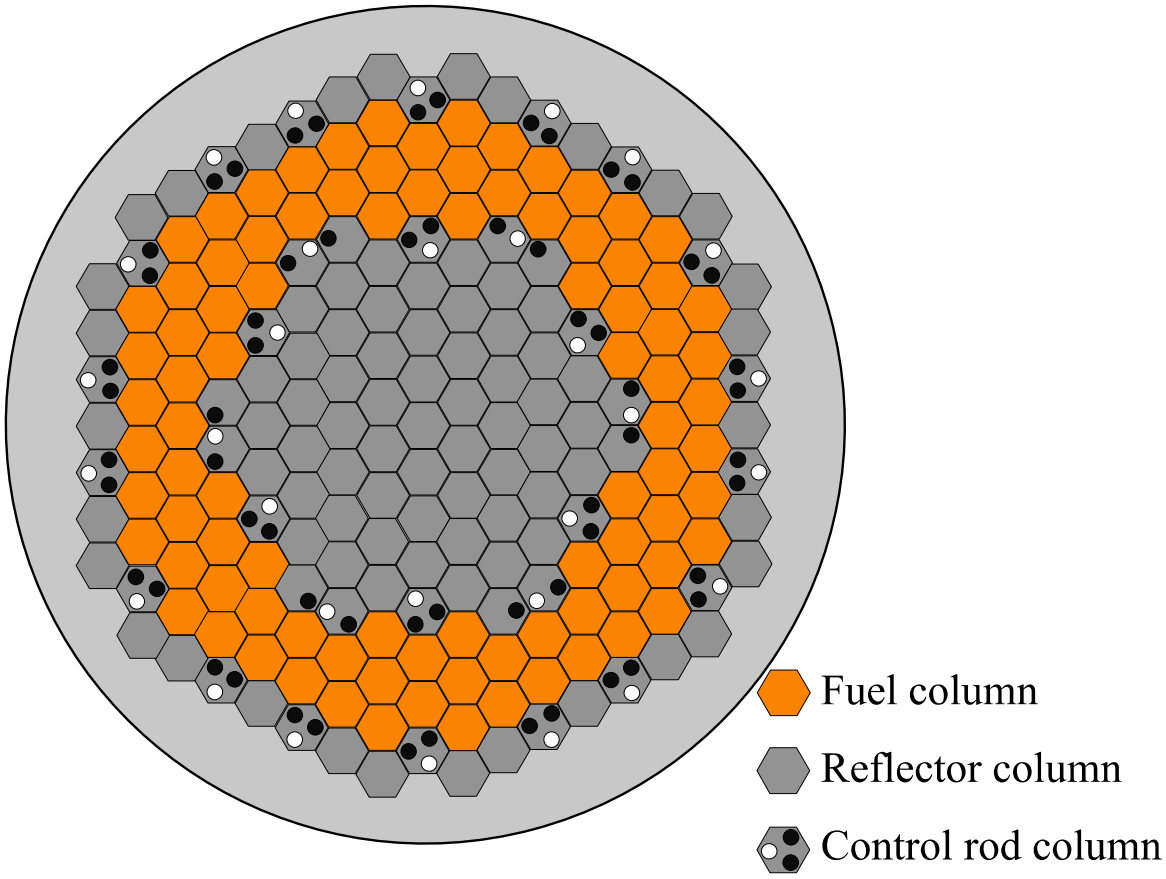


Fig.2 Geometry model for MVP calculation to generation ORIGEN library

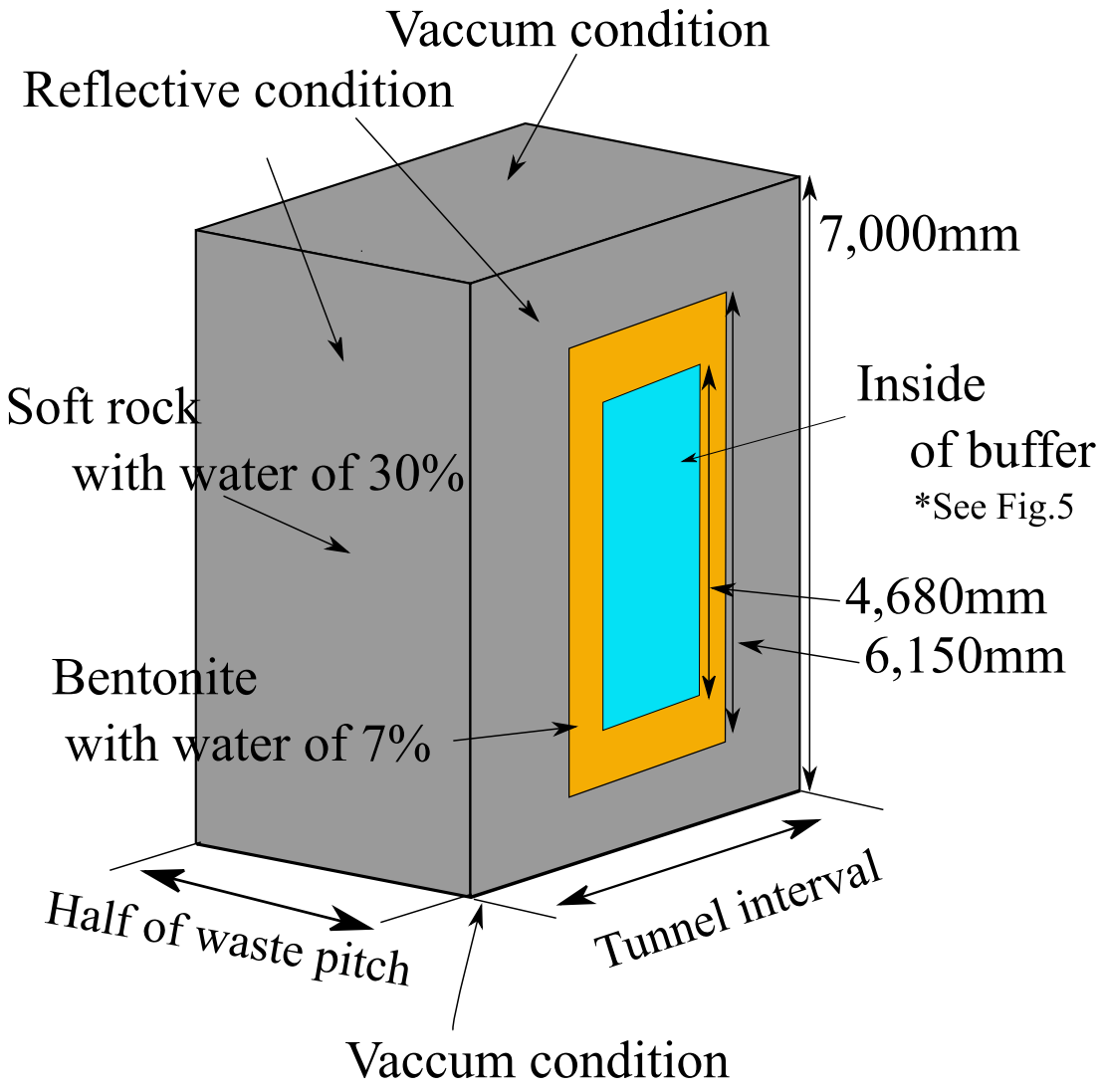


Fig.3 Geometry model for criticality calculation in repository

Y. Fukaya:
Reduction on High Level Waste and Geological Repository Footprint with High Burn-up and High Thermal Efficiency of HTGR

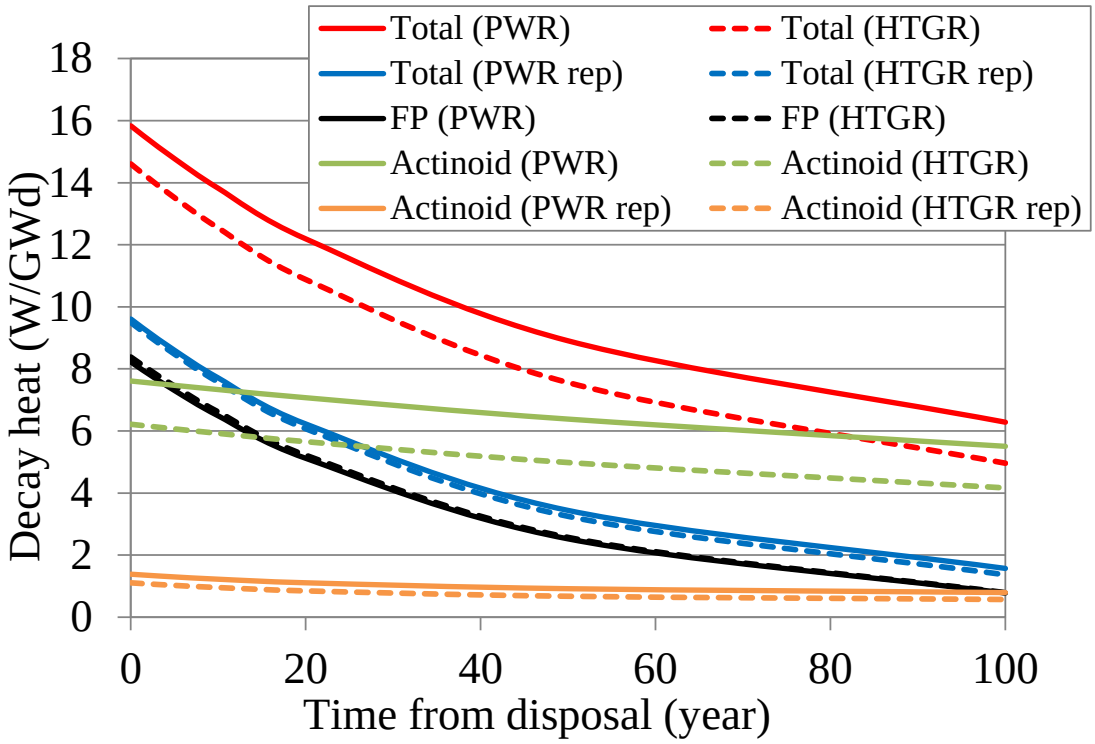


*rep stands for with reprocessing.

Fig.4 Decay heat per burn-up of PWR and HTGR

Y. Fukaya:
Reduction on High Level Waste and Geological Repository Footprint with High Burn-up and High Thermal Efficiency of HTGR

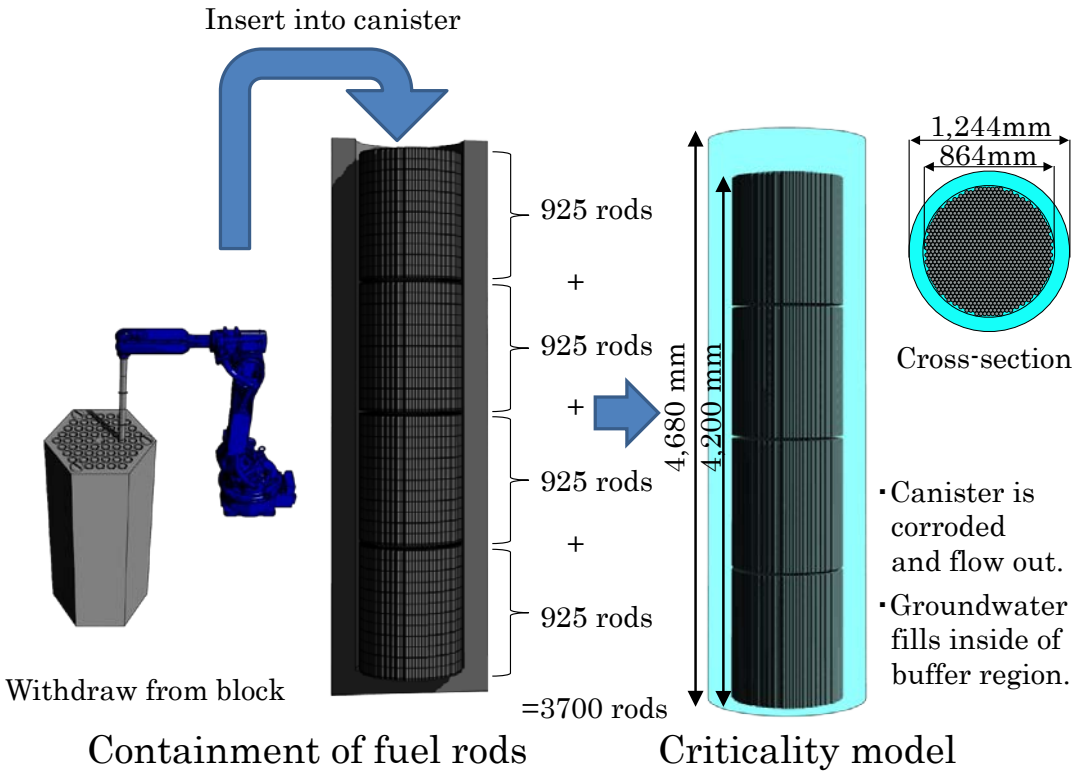


Fig.5 Proposed waste loading method for HTGR and its criticality model in repository

Y. Fukaya:
Reduction on High Level Waste and Geological Repository Footprint with High Burn-up and High Thermal Efficiency of HTGR

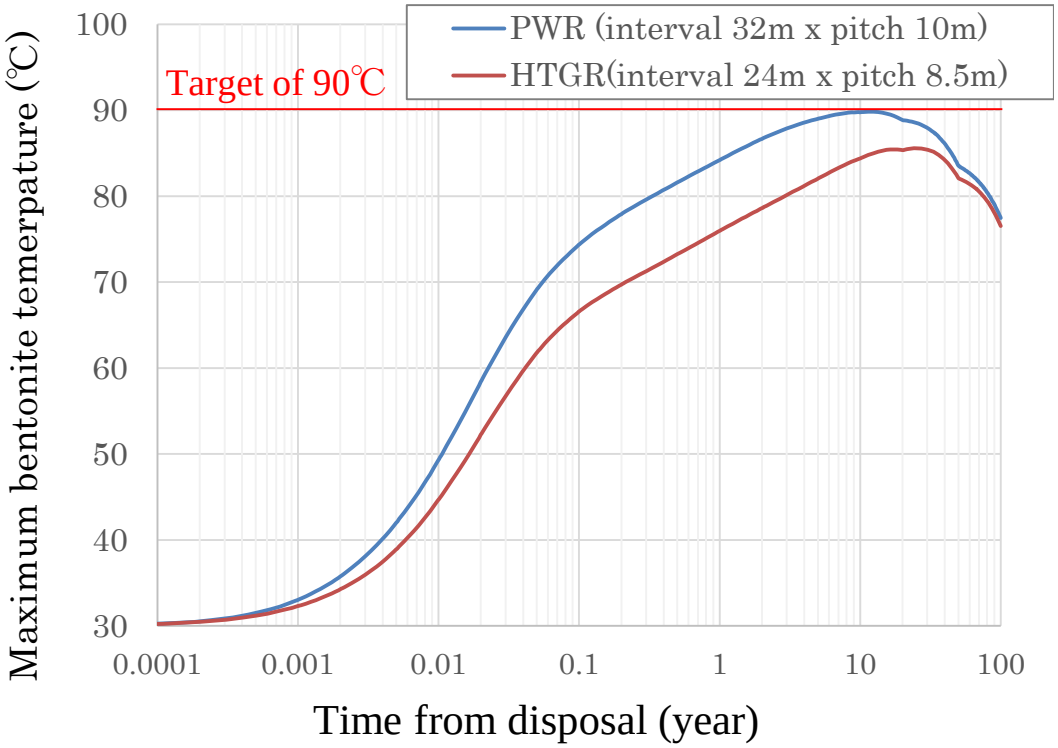


Fig.6 Maximum bentonite temperature during disposal

Y. Fukaya:
Reduction on High Level Waste and Geological Repository Footprint with High Burn-up and High Thermal Efficiency of HTGR

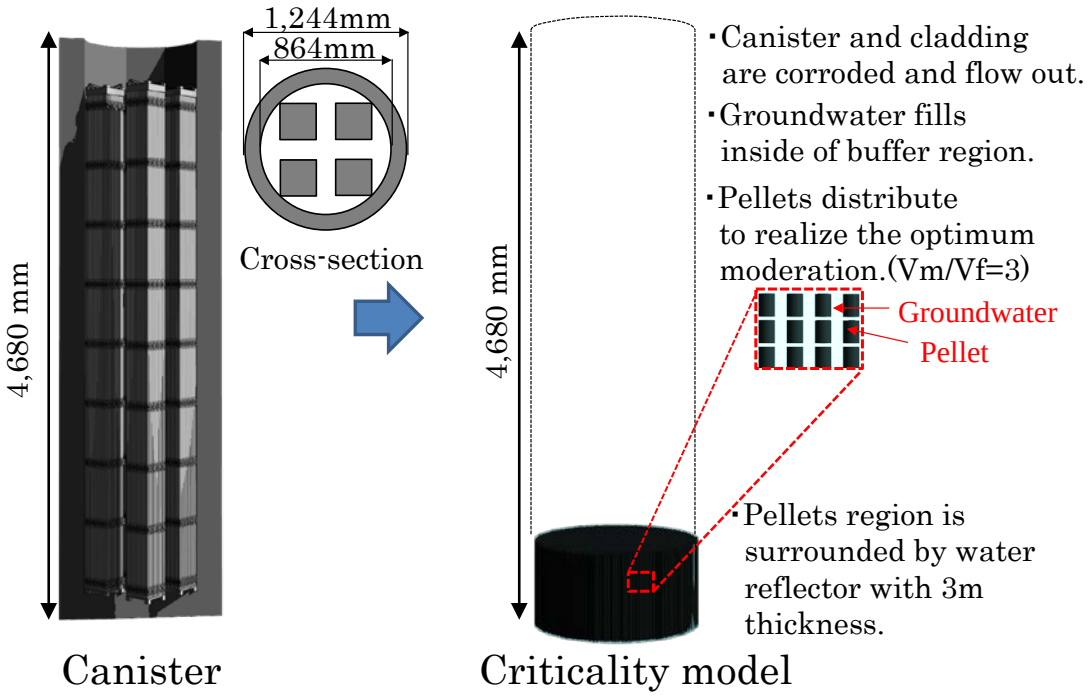


Fig.7 PWR canister and criticality model of JAEC

Y. Fukaya:
Reduction on High Level Waste and Geological Repository Footprint with High Burn-up and High Thermal Efficiency of HTGR

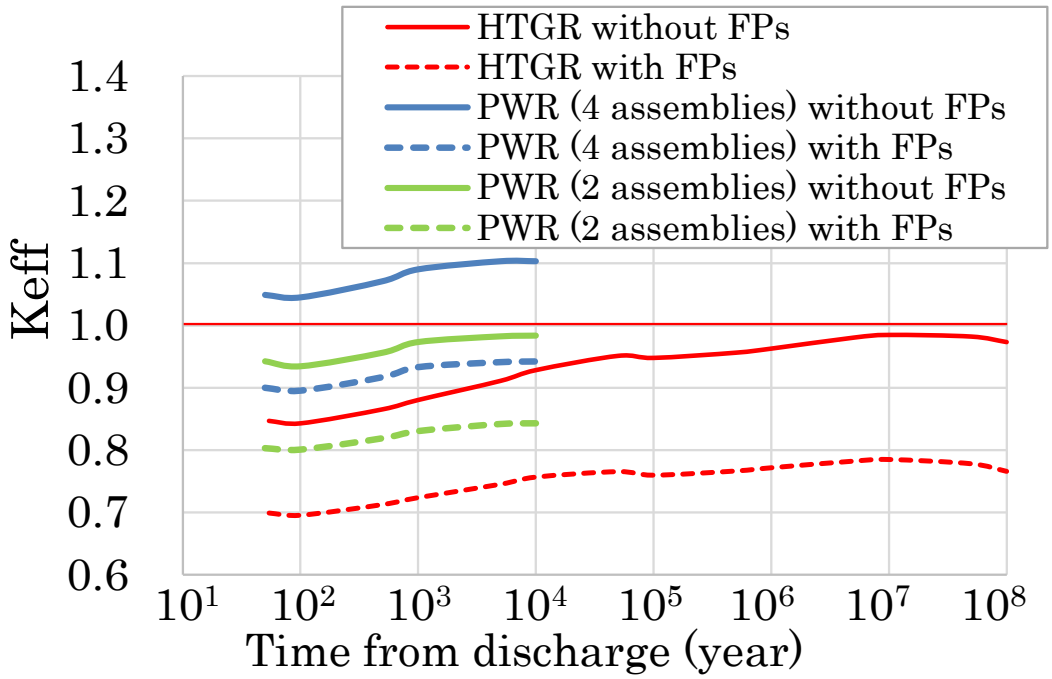


* The values of PWR are referred from the JAEC report.

Fig. 8 Criticality changes in repository

Y. Fukaya:
Reduction on High Level Waste and Geological Repository Footprint with High Burn-up and High Thermal Efficiency of HTGR